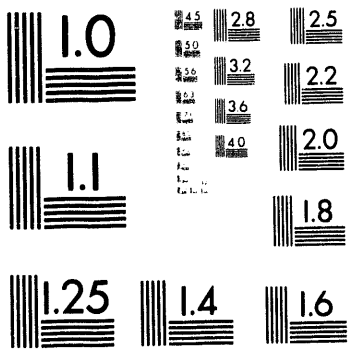
1.0
1.1
1.25
1.4
1.6
1.8
2.0
2.2
2.5
2.8
3.2
3.6
4.0
4.5
5.0
5.6

1 of 1

A SHUTTLE MECHANISM FOR MOLTEN-ELECTROLYTE LITHIUM BATTERIES

T. D. Kaun and P. A. Nelson
Argonne National Laboratory
Chemical Technology Division
Argonne, IL 60439-4837

ABSTRACT

The lithium-transport rates arising from a lithium shuttle mechanism (LSM) were examined by potentiometric control of a lithium-alloy electrode in a temperature range of 400 to 515°C in three electrolytes: LiCl-KCl, LiCl-LiBr-KBr, and LiF-LiCl-LiBr. Lithium transport in Li/FeS_x cells by LSM was found to occur by diffusion of reduced lithium species across the separator layer, which was controlled by the Li-activity of the Li-alloy electrode. Solubility of lithium was strongly affected by electrolyte composition, especially K^+ content, which in turn regulated the lithium transport rate. As evidenced by LSM rates, the solubilized lithium would appear to form dimers (e.g. Li_2^+ or LiK^+). The half-cell self-discharge rates, which were measured, correlate well with self-discharge rates in developmental cells ranging from 0.1 to 10 mA/cm^2. Innovative application of the LSM has led to the development of overcharge tolerant Li/FeS_x cells. A bimodal self-discharge characteristic (a 20-fold increase toward the end of charge) results from a 150-250 mV step increase in lithium activity of a two-phase Li-alloy electrode (Li-Al plus Li-Al_5Fe_2). Three versions of the battery cell (100 cm^2 separator area) have been demonstrated: LiAl+$Li_5Al_5Fe_2$(10% of capacity)/LiCl-LiBr-KBr(MgO)/FeS_2, as well as a FeS-type, (both operated at 400°C) and LiAl+$Li_5Al_5Fe_2$(10% of capacity)/LiF-LiCl-LiBr(MgO)/FeS (operated at 475°C). These cells exhibit a unique combination of overcharge capacity and extended trickle-charge tolerance at 2-5 mA/cm^2. Additionally, Li/FeS_2 cells having overcharge tolerance have operated with stable performance for greater than 500 cycles. The overcharge tolerance rates are sufficient for battery cells to exhibit built-in charge/equalization capability by way of full-battery trickle charging.

INTRODUCTION

Earlier Li/FeS_x battery cells (1) with molten electrolyte had required an electronic charger/equalizer (2) (necessitating a wire to each cell) to protect them from destructive overcharging. Overcharging generally results in oxidation of the current collector in the positive electrode (FeS or FeS_2). With an iron current collector, for example, this produces the undesirable reaction Fe→$FeCl_2$. This overcharge leads to shorted cells by deposition of iron particles within the separator. The development of Li/FeS_x cells which are inherently overcharge tolerant would eliminate the need for electronic safeguards and would aid battery development. An earlier innovation (3) resulted in cells that could be overcharged at full battery

charge current for a finite capacity (e.g., 10% of rated capacity). The development to be reported on here gives these cells an additional extended trickle-charge tolerance (4), which causes battery cells to approach an equal state of charge.

An understanding of self-discharge by lithium transport is also of general interest to the development of molten electrolyte batteries for both primary and secondary applications. Coulombic efficiency and length of allowable open-circuit stand time are important operating parameters. At high temperatures (>500°C), high lithium activity (near Li^0) gives rise to self-discharge rates that need to be actively managed. The dominant self-discharge mechanism depends upon a rate controlled by the activity of the Li-alloy electrode. The proposed "lithium shuttle" mechanism (LSM) involves: (1) dissolution of Li^0 (probably to form Li_2^+ or LiK^+) at the Li-alloy electrode surface, (2) diffusion of the Li^0 across the electrolyte/separator to the positive electrode, and (3) electrochemical discharge of the Li^0 to produce Li^+ at the positive electrode. We have investigated the parameters of Li-alloy electrode potential and temperature that control this mechanism in the three most commonly used electrolytes. In application, compact prismatic cells have demonstrated the effectiveness and long-term stability of the "lithium-shuttle" for overcharge tolerance. In an earlier study of self-discharge in LiAl/FeS cell without the benefit of reference electrodes, Knodler (5) presumed that electronic conductivity of the electrolyte is a controlling mechanism. However, our work indicates that a LSM more closely describes the observed self-discharge. The LSM explains >99% coulombic efficiencies in the normal operation as well as the much greater steady-state self-discharge rates attained for overcharge tolerance. The design of the overcharge tolerant cell is based on use of a Li-alloy electrode with two distinct states of lithium activity. This two-phase Li-alloy electrode establishes appreciably different rates of self-discharge for the cell. The higher rate is associated with the cell's overcharge capacity. This design approach for overcharge tolerance involving the LSM is tied to the Li-alloy electrode and, therefore, applies to cells with FeS or FeS_2 electrodes (6).

EXPERIMENTAL

The LSM was initially investigated by potentiometric measurements on a three-electrode cell within a helium-atmosphere glovebox. All three electrodes contain lithium alloy, and no sulfur activity was involved. They were contained in Type 304 stainless steel housings and Type 325 mesh face screening. A Li-alloy working electrode (either LiAl, Li_4AlSi, or $Li_5Al_5Fe_2$) of 0.31 cm^2 area was horizontally positioned versus a counter electrode of αAl + βLiAl of 10 Ah capacity in about 100g molten salt, which was held in an Al_2O_3 beaker. Eutectic compositions of either LiCl-KCl, LiF-LiBr-LiCl, or LiCl-LiBr-KBr were obtained from Anderson Physics Laboratory, Urbana, IL. The working electrode was positioned parallel to the counter electrode at a set distance, typically 1.50 mm. Using a PAR 173 potentiostat, potentials of the working electrode were maintained in the range of 0 to -270 mV versus an αAl + βLiAl reference electrode (30 at.% Li-Al at 0 mV, hereafter called "LiAl reference electrode"). The potential establishes a self-discharge rate by

lithium transport for a set of test conditions (temperature, electrolyte composition, electrode area, electrode separation). Temperature was controlled to ±2°C at five temperature settings: 400, 425, 465, 490, and 515°C. The self-discharge rate was examined by cyclic voltametry at a scan rate of 0.01 mV/s. Steady-state values taken at 25 mV increments for >1/2 h reproduced these self-discharge rates.

In the development of overcharge tolerant cells, both FeS and FeS_2 compact prismatic bicells were tested. The FeS_2 cells (25 Ah) had an MgO powder (Maglite S, Culigan) separator (100 cm^2 at full height) and were operated in the electrolyte-starved condition with LiCl-LiBr-KBr off-eutectic (LiCl-rich, 34:32.5:33.5 by mol%) electrolyte. After assembly in an argon-atmosphere glovebox, the cells were sealed with a packed AlN-powder feedthrough. Cells were generally charged at 25 mA/cm^2 and discharged at 50 mA/cm^2. More recently, disk-shaped monocells of uniform current distribution (3 cm and 13 cm dia., 0.5 and 25 Ah respectively) were evaluated for overcharge tolerance. The cells are fabricated at a 90% state of charge: LiAl + Al_5Fe_2 (negative electrode) vs. FeS_2 + Li_2FeS_2 (positive electrode). The uncharged positive electrode capacity is sufficient to form $Li_5Al_5Fe_2$ at the negative electrode before FeS_2 is fully-charged at the positive electrode. Thus, the negative-electrode limits charge capacity.

Overcharge tolerance in these Li/FeS_x test cells was evaluated by galvanic and coulometric methods. The test cells had two-phase Li-alloy electrodes which were designed to exhibit a bimodal, stepwise change in lithium activity. This bimodal character was accomplished by replacing approximately 10% of the lithium capacity of the LiAl electrode with $Li_5Al_5Fe_2$ (7). The Li-Al_5Fe_2 electrode's potential is -260 mV. Overcharge tolerance evaluation was conducted after about every 20 cycles during the cell test. The evaluation proceeded by establishing a trickle charge of 2 to 5 mA/cm^2 during which the Li-alloy electrode exhibited potentials vs. LiAl reference electrode that are associated with the $Li_5Al_5Fe_2$ electrode at -225 to -275 mV. Under cycling to various charge voltage cutoffs, cell coulombic efficiency also indicated self-discharge rates for the rated (normal) capacity and overcharge states. The overcharge tolerance rates in cells were determined coulometrically.

RESULTS AND DISCUSSION

Lithium-Shuttle Rate Measurements

The results of the potentiometric experiments elucidated the parametric control of the LSM and indicated the viability of developing full-scale Li-alloy/FeS_x cells with overcharge tolerance. Significant rates of self-discharge (up to 20 mA/cm^2) were established by polarizing a solid-particulate Li-alloy electrode in molten LiCl-KCl (58:42 mol%) for the temperature range of 400 to 515°C to near Li^0 potential. The lithium shuttle rate exhibits exponential dependence with Li-alloy potential and temperature. By a Henry's law assumption the lithium activity locally in the molten salt is proportional to the lithium activity of the Li-alloy electrode at a liquid/solid interface. The dependence of LSM with Li-alloy electrode potential and therefore lithium-activity is quite evident, with a 30-fold change over the potential range of 0

to -270 mV vs. LiAl reference. For all temperatures, appreciable LSM rates of 2-10 mA/cm^2 were attained at about -200 mV vs. the LiAl reference electrode. This potential is safely away from that for the deposition of liquid lithium. Also, the current density of the LSM is typical of cell capacity equalization rates for battery chargers. The Li-activity of Li-Al_5Fe_2 is well suited for establishing stable self-discharge rates for overcharge tolerance; the electrochemical potential at -260 mV is in the desired range and is stable with change in lithium composition. Also, this electrode does not form liquid alloy phases in the potential and temperature ranges of interest.

Our results indicate the lithium shuttle rate is controlled by the Li-alloy electrode potential for all three electrolytes over the full temperature range tested. The potential of the lithium electrode apparently sets the lithium concentration in a Fick's law diffusion process for lithium transport. Lithium flux away from the negative electrode is equal and opposite to the charge current necessary to maintain a steady state. Therefore, we can write a lithium flux equation in terms of a LSM current density:

$$i = FD\ [C_{0_{(T,E)}} - C_1](1 - f)^{1.5}/h \qquad [1]$$

where
- i = lithium shuttle rate, mA/cm^2
- F = Faraday's constant
- D = diffusion constant
- C_0 = lithium concentration at Li-alloy electrode related to temperature and electrode potential
- C_1 = lithium concentration at metal sulfide electrode
- $(1 - f)^{1.5}$ = electrolyte fraction in separator, with Bruggeman exponential factor
- h = thickness of separator

Lithium at the face of the metal sulfide electrode reacts rapidly, so C_1 is assumed to be zero.

Figure 1 presents self-discharge rates measured in the three electrolytes at a set of conditions with temperatures of 425 and 490°C, respectively. Figure 1(a) has only two electrolytes because 425°C is below the melting point of LiF-LiCl-LiBr. At the lower temperature, self-discharge rates are almost negligible until -200 mV. At 50-100°C higher temperatures, self-discharge rates at -200 mV rise to 10-20% of typical operation current density. Independent of the temperature and electrolyte composition effects, the LSM increases by about a factor of 10 from 0 to -200 mV, and then doubles for a -200 to -250 mV potential change. The dominance and consistency of Li-alloy electrode potential to control LSM gives the basis for designing overcharge tolerance. Fortunately, Li-alloy electrode potential is the most easily changed variable during cell operation. One has little flexibility in controlling other variables, such as separator properties, electrolyte composition, and temperature, during cell operation. Therefore, based on an anticipated electrolyte

composition and operating temperature, one can adjust the Li-alloy electrode composition (lithium activity) to achieve the desired LSM for overcharge tolerance and yet maintain ≥90% of cell capacity at negligible self-discharge rates (4).

The molten electrolyte composition is an important factor in establishing the working range of a cell's lithium shuttle rate. As can be deduced from Fig. 1 at a given temperature, self-discharge rates increase almost linearly with the K^+ content of the molten electrolyte (whereas temperature and Li-activity cause exponential changes). The lithium transport rate at five temperatures is plotted in Fig. 2. This Arrhenius plot at -250 mV provides a key insight into the "lithium-shuttle" mechanism based on lithium transport by diffusion. As shown in Fig. 2, the lithium shuttle rate for the K^+-containing electrolytes is higher and has greater temperature dependence than that for the all-Li^+ electrolyte. The lithium transport rates established by the different electrolytes can be fit to an Arrhenius equation. As indicated in Table 1, Arrhenius coefficients for the K^+-containing electrolytes are more than 10 fold greater than those of the all-Li^+ electrolyte, while the activation energies for Li transport (and possibly K) are only about 1/3 greater. The extent of lithium solubility is apparently greater in K^+-containing electrolytes but still needs to be determined for other electrolyte compositions. Earlier measurements of lithium solubility (8) indicated levels in LiCl-KCl almost double those in LiCl. These levels of dissolved metal are on the order of 0.1 to 0.2 mol% when projected to 400 to 500°C (9). Therefore, the rate constants of lithium transport indicate lithium solubility for a given molten salt composition, whereas the activation energies indicate the solvation of the lithium molecule.

A projection of the all-Li^+ electrolyte data to lower temperatures indicates rates similar to the K^+-containing electrolytes. It follows that more energy would be required in the transport of the lithium molecule solvated with the larger K^+ ion. The following electrochemical reactions leading to lithium dissolution are proposed for K^+-containing and K^+-free electrolytes, respectively:

$$Li^+ + K^+ + e^- \rightarrow LiK^+ \qquad [2]$$

and

$$2Li^+ + e^- \rightarrow Li_2^+ \qquad [3]$$

The lithium activities and the Gibbs free energy of mixing of dissolved lithium with LiCl-KCl and LiCl were determined by Smirnov and Podlesnyak (8). Their data support the formation of LiK^+ subion for the K^+-containing molten salts rather than Li_2^+. To a lesser extent, a dual mechanism of K and Li transport for self-discharge in the K^+-containing electrolyte is also possible. All three molten electrolytes exhibit quite similar exponential increases in self-discharge rates with temperature (i.e., activation energy). This observation again suggests that the electrolyte composition imposes limits upon lithium transport rate related to the level of lithium solubility. Since the potential sets the lithium activity at the lithium-alloy electrode, the increased rates of LSM for the K^+-containing electrolytes implies, by Fick's law, that the diffusion of lithium across the separator is not limiting but rather the levels of

lithium solubility (or supplemental potassium solubility) in the molten salt. In other words, the electrolyte composition affects the diffusion constant by dictating the composition of the solvated lithium molecule.

An alternative description of self-discharge involves electronic conductivity of molten LiCl-KCl which has been measured as a function of lithium activity by Reynolds et al. (10). Their reported values of self-discharge rates are a factor of 10 less than those reported here from lithium transport. Further, with C_1 approximated as zero at the sulfide electrode face, electronic conductivity in the electrolyte would be very low or discontinuous. In addition, the LSM conforms to the definition of dilute solution of metal in molten salt, which falls into the "non-metal" solution classification of Bredig et al. (11). As such, the solvation of the lithium molecule to form the dimers of LiK^+ or Li_2^+ further curtails electronic conductivity from dissolved lithium. Therefore, self-discharge by electronic conductivity in the electrolyte would not seem to explain, by itself, the rapid response to Li-electrode potential that is seen. In another paper, we proposed a model combining the two phenomena (12). There, relative contributions of lithium transport and electronic conductivity is postulated to vary across the electrolyte/separator thickness.

The lithium shuttle rate is reasonably well explained by lithium flux in the molten-salt electrolyte. By Faraday's law, it is related to current density, and with $C_1=0$ we can write

$$i = FD\ C_{0_{(T,E)}}(1 - f)^{1.5}/h \qquad [4]$$

Here, C_0 strongly determines the rate of lithium flux as related to electrode potential and solubility of lithium in the molten salt. The lithium solubility depends on molten-salt composition related to K^+ concentration. In this regard, the molten-salt composition changes the solvated form of the lithium molecule, Li_2^+ or LiK^+. As a result, the activation energy for lithium transport in the K^+-free electrolyte is significantly lower. The rather large increase in lithium transport as a function of temperature implies changes in the solvated form of the lithium molecule with temperature in various molten-salt compositions. The local concentration of lithium at the Li-alloy electrode, C_0, equilibrates rapidly with changes in lithium electrode potential. The diffusion constant for lithium transport has a lesser effect upon the LSM. Based on these results, we calculated a diffusion constant of 1.35×10^{-5} $mol \cdot cm \cdot s^{-1}$. This reasonable value for a lithium diffusion constant in molten salt lends support to a LSM by lithium transport across the separator.

Development of Overcharge Tolerant Cells

A Li-alloy electrode exhibiting bimodal lithium activity has been developed to provide overcharge capacity, as well as overcharge tolerance, using the LSM. Figure 3 shows the potential vs. capacity for a 25-Ah LiAl electrode in which 10% of its lithium capacity (overcharge capacity) has been substituted by $Li_5Al_5Fe_2$. This two-

phase Li-alloy electrode has a decreased potential of -190 to -240 mV over its last 10% of charge. The open-circuit potentials may be 10 mV more negative under trickle charge rates. As the above results suggest, a cell using this Li-alloy electrode should exhibit increased self-discharge related to the high lithium activity, which imparts overcharge tolerance. A coulometric assessment of a Li-alloy/FeS_2 cell with the two-phase Li-alloy electrode reveals the LSM rate change. The cell (1.8 mm thick separator) is charged to voltage cutoff (2.05 V) and discharged in Cycle 1. Its coulombic efficiency at 425°C indicates a 0.15 mA/cm^2 self-discharge rate. Cycle 2 includes a 3-h trickle charge at 3.5 mA/cm^2 near full-charge state. The reduced coulombic efficiency indicates a 3.0 mA/cm^2 self-discharge rate (LSM) during the trickle-charge period. As the cell reaches full charge, at greater than 2.00 V, the two-phase Li-alloy electrode has transitioned to a 200 mV to 250 mV more negative potential. In confirmation of the increased LSM rate during trickle-charge, both cycles 1 and 2 yield the same discharge capacity.

Figure 4 plots the voltage during the charge half-cycle, along with the associated self-discharge rate for an overcharge-tolerant FeS_2 cell operated at 415°C in the upper-voltage plateau (U.P.). The bimodal self-discharge rate of the cell is coupled with a transition in its voltage/capacity curve. As the cell begins its transition into the overcharge capacity state, the self-discharge rate increases in a stepwise fashion by 20-fold, to about 2.5 mA/cm^2. In the overcharge state, the cell exhibits voltage and self-discharge characteristics relative to the $Li_5Al_5Fe_2$ constituent of the lithium electrode versus the U.P. FeS_2 electrode. Consistent with a typical 2.00 V charge cutoff, the bimodal character of the two-phase Li-alloy electrode yields a cell with a unique combination of overcharge capacity and overcharge tolerance.

The overcharge capacity safeguards the cell and permits unmonitored bulk charge at 20-50 mA/cm^2 with a battery voltage limit. A battery can thus be charged with a voltage that is 2.00 V multiplied by the number of cells in the battery (e.g., a 100-cell battery would be charged at 200 V). Assuming a bell-shaped distribution in charge capacity acceptance of cells at completion of a bulk charge, the "stronger" half of the battery cells would attain the overcharge capacity state. (The conventional electronic charger/equalizer, which monitors the voltage of each cell, would have ended the bulk charge when the first cell attained a charge cutoff voltage of 2.00 V). After the bulk charge, battery cell equalization is accomplished by a battery trickle charge of about 2.5 mA/cm^2. The "stronger" cells, which have been safeguarded by the overcharge capacity, are charged at approximately 0% coulombic efficiency because the trickle-charge rate balances the lithium-shuttle rate. The "weaker" cells, on the other hand, accept additional capacity at about a 2.5 mA/cm^2 rate over a 3-6 h period and undergo an additional 5-10% increase in capacity. The battery is effectively charge equalized when all the battery cells have reached the overcharge capacity state (without any electronic monitoring). Figure 5 provides the voltage/time plots of a small battery (four overcharge-tolerant cells connected in series) which has been operated to a battery voltage cutoff. A subsequent charge includes a trickle charge period near full-charge state. As a result of the LSM, the

battery capacity has been increased, the strongest cell has not been jeopardized by overcharge, and weakest cell has increased in capacity.

The overcharge-tolerant FeS cells at 475°C with the two-phase Li-alloy electrode have demonstrated even higher rates of overcharge tolerance, 3-5 mA/cm^2. [Overcharge tolerance has also been measured for a LiAlSi/FeS couple (13).] These cells were operated at higher temperature, 475-500°C, and with an all-lithium electrolyte. The higher temperature increases the LSM rate to counter balance the lower lithium solubility of the all-lithium electrolyte.

The overcharge-tolerant cell has demonstrated long-term stability (500 cycles) with high performance for both types of Li-alloy/FeS_x cells. The U.P. FeS_2 cell (operated only on the upper voltage plateau for the $FeS_2 \rightarrow Li_2FeS_2$ discharge) maintained a capacity that is at least 80% utilization of the U.P. FeS_2 electrode, which is typical for these cells (14), for over 225 cycles (3000 h). Additionally, the bimodal self-discharge rate characteristic maintained 2.0-2.5 mA/cm^2 overcharge tolerance levels with cycling. The MgO separator demonstrated chemical stability to high lithium activity, as indicated by ≥98% coulombic efficiency for cycles at rated capacity. Disk-cells with uniform current-distribution as in stacked configuration have operated 500 cycles. The high lithium-activity of overcharge tolerant cells spurred development of new ceramic materials. In two separate instances (different FeS cells), a feedthrough short circuit occurred coincidental with high O_2 content (~1.0%) in the glovebox atmosphere. Earlier investigations (15) indicated that the BN in the feedthrough became conductive under prolonged exposure to high lithium activity (near Li^0). The BN powder packing was replaced by other materials (AlN, MgO). The cells continued operation after the feedthrough was rebuilt. Currently, the use of AlN powder feedthrough packing has demonstrated extended cycle-life. Ongoing seal development for Li/FeS_2 cells use a fusible sulfide ceramic sealant (16), which likewise exhibits long-term (>500 cycle, 2000 h) stability within the high lithium activity environment. This new ceramic sealant has been applied to 1-cm dia feedthroughs, as well as 13-cm ID ring seals.

CONCLUSIONS

An understanding has been gained of the controlling parameters for the LSM, which involves diffusion transport of reduced lithium species (and possibly potassium). Our potentiometric measurements indicate that both Li-alloy electrode potential (lithium activity) and temperature exponentially increase self-discharge rates--up to approximately 20 mA/cm^2 for operation at 515°C and -270 mV. Moreover, a change in potential of the Li-alloy electrode from 0 to -270 mV at a given temperature increased self-discharge by 30 fold. LSM rates increase proportionally to the K^+ content of the molten electrolyte for the three electrolytes studied. The development of rate expressions for Arrhenius coefficients and activation energies provided insight into the effect of electrolyte composition upon lithium transport. The electrolyte composition strongly influences rate of lithium transport by its effect on lithium solubility. Further investigation of lithium

solubility and identification of lithium solvated forms would help to better model the LSM.

As confirmed by our potentiometric measurements, the sustained LSM rates demonstrated in representative test cells were sufficient for the development of overcharge-tolerant Li-alloy/FeS_x cells. A key development has been the operation of a two-phase Li-alloy electrode (Li-Al and Li-Al_5Fe_2), which establishes a bimodal self-discharge rate for the cells; a 20-fold increase in self-discharge occurs in the overcharge capacity state for cells designed with overcharge tolerance. The U.P. FeS_2 cell, operated at 400-425°C with LiCl-LiBr-KBr electrolyte, sustained overcharge tolerance rates of 2-3 mA/cm^2. The FeS cell, operated at 475-500°C with LiF-LiCl-LiBr electrolyte, sustained overcharge tolerance rates of 3-5 mA/cm^2. In ongoing testing, both types of cells demonstrated cycle-life stability in excess of 200 cycles (life expectancy is greater than 1000 cycles). In conclusion, overcharge-tolerant Li/FeS_x cells will enable charge capacity equalization of battery cells without need for equalization electronics. The bimodal lithium shuttle rate allows a "weaker" cell to accept trickle-charge capacity at high efficiency, while cells in an overcharge state assume a static state-of-charge.

ACKNOWLEDGMENT

This work was done under the auspices of the U.S. Department of Energy, Energy Systems Storage Branch, under contract W-31-109-Eng-38. The authors are grateful for the support of D.R. Vissers, G.L. Henriksen, and K.M. Myles.

REFERENCES

1. T. D. Kaun, L. Redey, and P. A. Nelson, "Molten-Salt Battery Advances," Proc. of 22nd IECEC, Philadelphia, PA, pp. 1085-1090 (1987).
2. W. H. DeLuca, A. A. Chilenskas, and F. Hornstra, Proc. of 14th IECEC, "A Charging System for the LiAl/FeS Electric Vehicle Battery," Aug. 5-10, 1979, Boston, MA, p. 660, Amer. Chem. Soc. (1979).
3. T. D. Kaun and A. A. Chilenskas, U.S. Patent 4,324,846 (1982).
4. T. D. Kaun and P. A. Nelson, U.S. Patent No. 4,851,306 (1989), and L. Redey and P. A. Nelson, U.S. Patent No. 4,849,309 (1989).
5. R. Knodler, J. Electrochem. Soc. 130, 16 (1983).
6. T. D. Kaun, P. A. Nelson, L. Redey, D. R. Vissers, and G. L. Henriksen, Electrochemica Acta. 38, 1269 (1993).
7. T. D. Kaun, U.S. Patent 4,158,720 (June 19, 1979).
8. M. V. Smirnov and N. P. Podlesnyak, Zhuv. Priklad. Khim 43, 1463 (1970).
9. V. A. Maroni, R. D. Wolson, and G. E. Staahl, Nuc. Tech. 25, 83 (1975).
10. G. J. Reynolds, M. C. Y. Lee, and R. A. Huggins, Proc. of 4th Int'l. Symp. on Molten Salts, p. 579, Vol. 84-2, The Electrochemical Society (1984).
11. M. A. Bredig, in Molten Salt Chemistry (edited by M. Blander), Interscience, New York, p. 367 (1964).

12. T. D. Kaun and P. A. Nelson, Extended Abstracts, AIChE Meeting, Chicago, IL, Nov. 11-16, 1990, p. 221 (1990).
13. L. Redey, J. Electrochem. Soc. 136 (7), 1989 (1989).
14. T. D. Kaun, T. F. Holifield, and W. H. DeLuca, "Lithium/Disulfide Cells Capable of Long Cycle Life," Proc. for the Materials and Processes for Lithium Batteries Symp., Ed., K.M. Abraham, Electrochem. Soc., Vol. 89-4, p. 373 (1989).
15. R. A. Sharma and T. G. Bradley, J. Electrochem. Soc. 128, 1835 (1981).
16. T. D. Kaun, U.S. Patent 5,162,172 (1992).

Table I. Arrhenius Coefficients (A) and Activation Energies (E_a) for Lithium Transport Rate Constants (k) in Molten Salts (400-515°C) as $k = Ae^{-E_a/RT}$

Electrolyte	Mol%K^+	A at -200 mV	A at -250 mV	$-E_a$ at -200 mV	$-E_a$ at -250 mV
LiCl-KCl	42	$3.29x10^5$	$1.55x10^9$	26.15	28.6
LiCl-LiBr-KBr	38	$8.22x10^5$	$8.73x10^8$	28.25	28.06
LiF-LiCl-LiBr	0	$1.33x10^3$	$7.1x10^7$	19.90	22.0

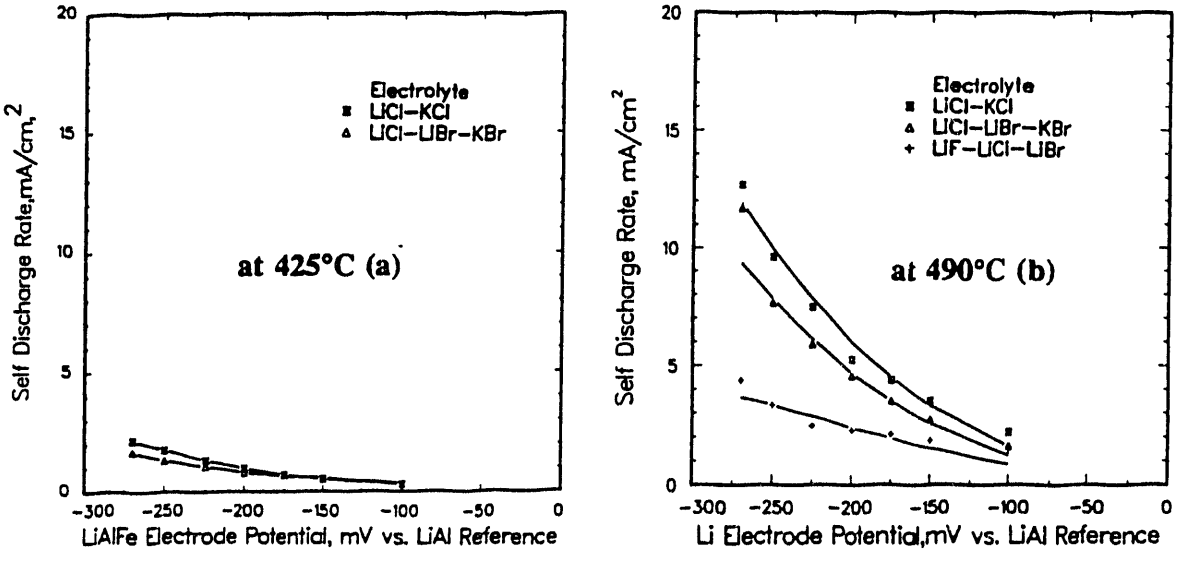

Fig. 1 Self-discharge rates vs. potential of lithium-alloy electrode in various molten-salt electrolytes at 425°C (a) and at 490°C (b)

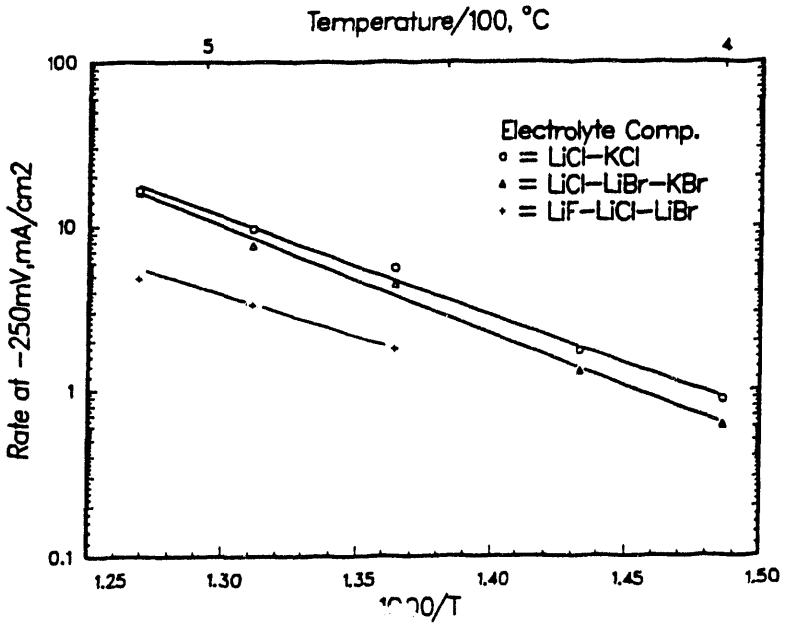

Fig. 2 Effect of temperature upon lithium shuttle rates at about -250 mV vs. LiAl reference electrode in three molten-salt electrolytes

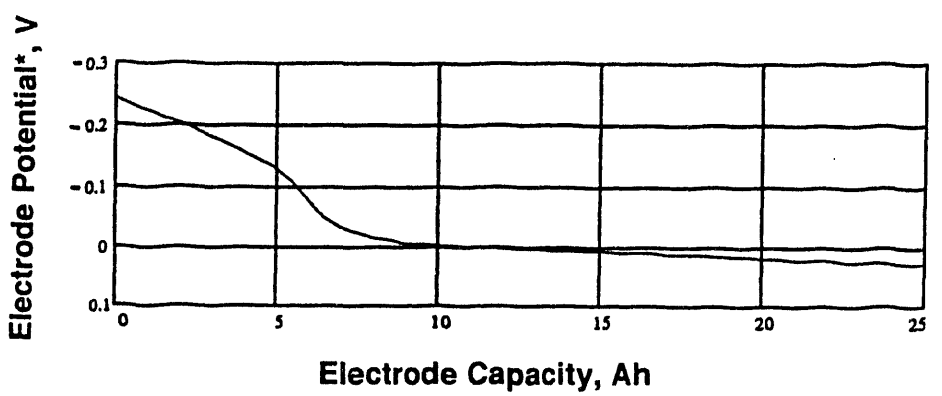

* Potential vs. LiAl Reference Electrode, 25 at%, Li-Al during charge half-cycle

Fig. 3 Electrode potential vs. charge capacity of two-phase Li-alloy electrode, 90% Li-Al + 10% Li-Al_5Fe_2 (25-Ah) in LiCl-LiBr-KBr at 425°C

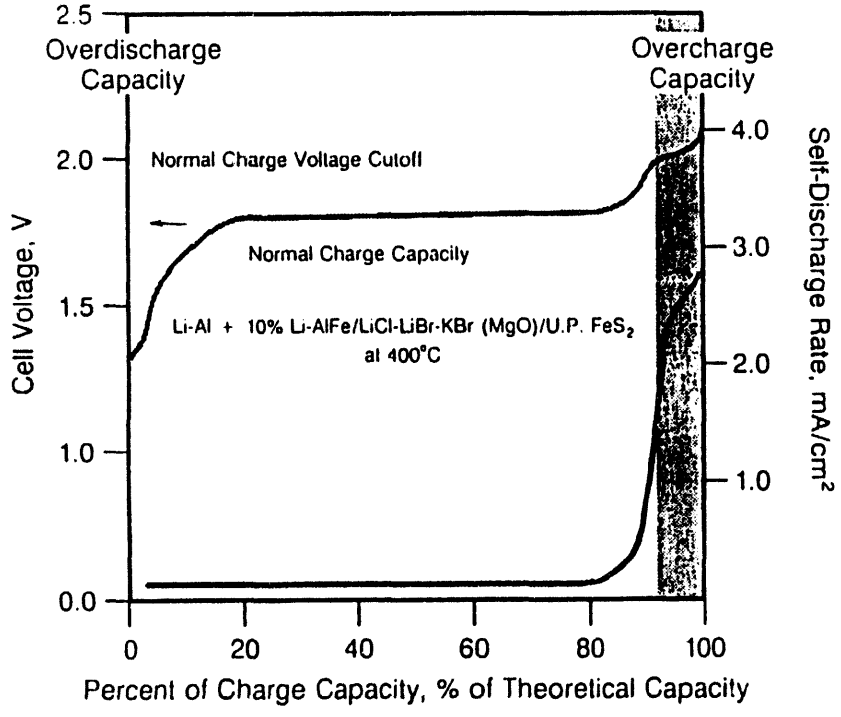

Fig. 4 **Li/FeS_2 cell self-discharge rate as related to state of charge, LSM rate increased due to increased lithium electrode activity in overcharge capacity**

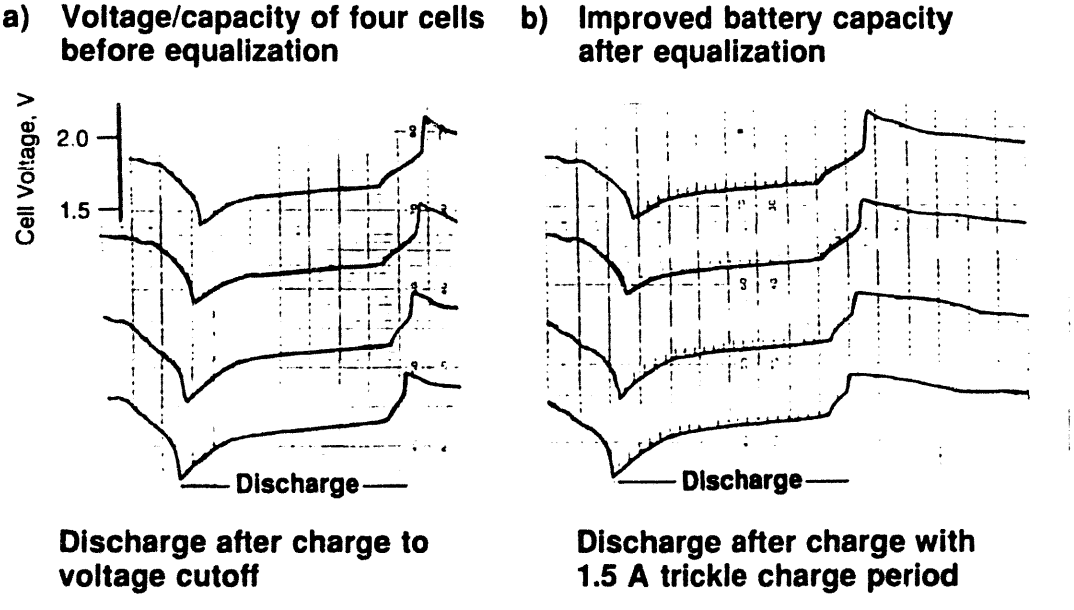

Fig. 5 **Two successive voltage/time plots of a four-cell Li/FeS_2 battery, illustrating battery equalization by trickle charging the battery**

DATE
FILMED
1/21/94
END